The Multiscale Medial Response of Grey-level Images

Ming Xu and David Pycock
School of Electronic and Electrical Engineering
University of Birmingham, Birmingham B15 2TT, UK
[xum|pycockd]@eee.bham.ac.uk

Abstract

The Concordance-based Medial Axis Transform (CMAT) presented in this paper is a multiscale medial axis (MMA) algorithm that computes medial evidence from grey-level boundary measures. It differs from previous algorithms of this type in considering the symmetry of both boundary position and strength. The resultant MMA transform is not prone to the generation of spurious medial responses exhibited by previous algorithms, but accurately estimates the position of the medial axis across scale. In addition, the medial axis and object scale are more distinctly identified. Thus CMAT medialness responses are easier to interpret than responses from previously reported measures. This is illustrated using a test figure and a radiograph of a hand.

1 Introduction

The medial axis is a structure, first proposed by Blum [1], that captures global shape properties of an object. It is defined as the locus of centres of the maximal disks that fit within an object. However, this single scale definition of the medial axis is sensitive to small variations in the boundary description of an object. To construct a robust medial axis representation, a hierarchy and thus a series of resolution reduction steps are usually needed. One approach is to smooth the segmented contours of objects. An alternative approach is to apply progressively larger blurring filters to images producing a set of scale-space images. Koenderink [4] argued that this approach captures global relationships better than contour smoothing. Moreover, this approach does not need a prior segmentation and avoids discarding important boundary information at an early stage of processing. Pizer's Multiscale Medial Axis (MMA) [6] is one such method. It has been successfully used in image registration [3] and object characterisation [7].

The MMA theory recognises that geometric measurements, such as medial axis computation, should be computed at scales (smoothing levels) proportional to the size of the object of interest. This allows the interpretation of fine-scale detail to be separated from the interpretation of larger-scale shape properties. Fritsch [3] convolved different sizes of LoG kernels with grey-level images to generate a "medialness" image and defined "medialness" as a measure of the likelihood that a given location is a symmetric point at that scale. The multiscale medial axis is a ridge in this medialness space. This definition of the MMA is a further extension to the multi-resolution scheme of Crowley and Parker [2], in which the DoG kernel is used. They both use an axis-centred operator

BMVC 1998 doi:10.5244/C.12.23

that responds well at a scale and position where the operator optimally engages two sides of an object. The Hough-like Medial Axis Transform (HMAT) [5] uses a boundary-centred operator, the first derivative of Gaussian, to measure "boundariness" in scale-space. These boundariness estimates are used to accumulate medialness responses at a distance from the boundary that is proportional to scale. As in [3], the ridge of the medialness response is the multi-scale medial axis. However, the medialness response obtained using the LoG and HMAT is like a propagation of boundary description and produces many spurious medialness responses which do not represent any true medial structure. Although the medialness values at "true" medial points are usually higher than those at neighbouring positions and scales it can be difficult, especially in noisy images and images that contain multiple figures, to identify the true medial response. In the LoG and HMAT, a strong isolated edge will make a strong contribution to the score in medialness space.

In this paper, we propose a Concordance-based Medial Axis Transform (CMAT), which considers the confidence of mutual support from multiple boundaries for a particular medial structure. The CMAT avoids spurious medial responses, provides an accurate localisation of the medial response and clearly identifies the scale of a symmetry.

2 Principle of CMAT

Each boundary point makes a vote proportional to its gradient magnitude. These votes are accumulated in medialness space at a distance from the boundary to provide an initial estimate of medialness. The accumulated value of the initial medialness estimate is not less than the value of any single vote. Only in positions where the initial medialness estimate is greater than the value for a single vote, is there evidence for true medialness. The confidence, that a boundary point is a part of a symmetric structure, can be judged from the ratio between the total votes from other boundaries and the initial medialness estimate at the relevant point in medialness space. The boundariness contribution to true medialness is proportional to its gradient magnitude as well as its confidence of symmetry. The medialness is the accumulation of these boundariness contributions.

3 Computation of CMAT

3.1 Boundariness

The first step is to produce the boundariness scale-space of the image, $I(\mathbf{x})$ using:

$$\mathbf{B}(\mathbf{x},\sigma) = I(\mathbf{x}) * \nabla G(\mathbf{x},\sigma) \tag{1}$$

where $\mathbf{x}$ is the spatial position, G is the Gaussian convolution kernel, and σ is the standard deviation of the convolution kernel G. For each point $\mathbf{x}_B$ in boundariness space its corresponding contribution at position $\mathbf{x}_A$ in medialness space is:

$$m(\mathbf{x}_A,\sigma) = \left\|\mathbf{B}(\mathbf{x}_B,\sigma)\right\| \tag{2}$$

Position $\mathbf{x}_A$ in the medialness space is defined as:

$$\mathbf{x}_A = \mathbf{x}_B + r\mathbf{B}(\mathbf{x}_B,\sigma) / \left\|\mathbf{B}(\mathbf{x}_B,\sigma)\right\| \tag{3}$$

where $r = k\sigma$ (k is a constant of proportionality with a typical value 2) (see Fig. 1).

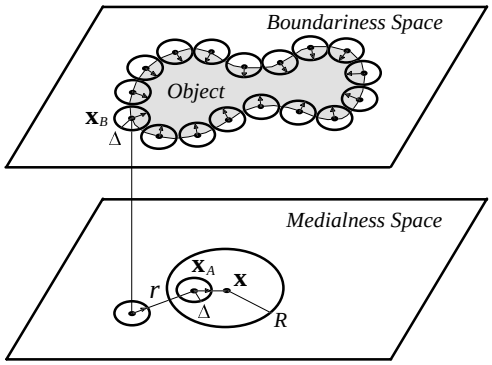

Figure 1: The boundariness contribution of point $\mathbf{x}_B$ is located at point $\mathbf{x}_A$ in medialness space. The confidence of mutual support is estimated by examining two elemental regions with radius Δ, centred at $\mathbf{x}_B$ and $\mathbf{x}_A$. The medialness response at point $\mathbf{x}$ is the integration of true contributions over a circular region with a radius of R .

3.2 Contribution of Boundariness to True Medialness

We define a measure of mutual support for each point $\mathbf{x}_B$, in boundariness space, in terms of the proportion of medialness evidence at position $\mathbf{x}_A$ provided by other boundary points as:

$$\text{mutual support } (\mathbf{x}_\mathrm{B}) \propto \frac{\text{medialness } (\mathbf{x}_A) - \text{boundariness } (\mathbf{x}_B)}{\text{medialness } (\mathbf{x}_A)}$$

When several boundary points from a symmetric structure contribute towards medialness, each contribution will be located at a tightly clustered set of real valued co-ordinates. The above medialness estimate is obtained by integrating over a small elemental area. To maintain consistency between the medialness and boundariness measure, the boundariness estimate is also integrated over an elemental area of the same size. The confidence of mutual support is defined as:

$$p(\mathbf{x}_B, \sigma) = \frac{\Delta m(\mathbf{x}_A, \sigma) - \Delta b(\mathbf{x}_B, \sigma)}{\Delta m(\mathbf{x}_A, \sigma)} \tag{4}$$

where:

$$\Delta b(\mathbf{x}_B, \sigma) = \int_{O^{\Delta}_{\mathbf{x}_\mathrm{B}}} \left\| \mathbf{B}(\mathbf{x}_B + \mathbf{u}, \sigma) \right\| d\mathbf{u} \tag{5}$$

$$\Delta m(\mathbf{x}_A, \sigma) = \int_{O^{\Delta}_{\mathbf{x}_\mathrm{A}}} m(\mathbf{x}_A + \mathbf{u}, \sigma) d\mathbf{u} \tag{6}$$

Here $O^{\Delta}_{\mathbf{x}_B}$ represents an elemental region circumscribed by a circle centred at position $\mathbf{x}_B$ with a radius Δ, and $O^{\Delta}_{\mathbf{x}_A}$ represents a similar region centred at $\mathbf{x}_A$. For an elemental area, $\Delta b(\mathbf{x}_\mathrm{B}, \sigma) \le \Delta m(\mathbf{x}_\mathrm{A}, \sigma)$. Therefore $0 \le p(\mathbf{x}_B, \sigma) \le 1$.

For discrete spatial sampling, boundary points are always located at sampling grids, but their contributions are not. A square-shaped elemental region with $\Delta = 0.5$ pixel is used. Therefore:

$$\Delta b(\mathbf{x}_B, \sigma) = \left\| \mathbf{B}(\mathbf{x}_B, \sigma) \right\| \tag{7}$$

The boundariness contribution to true medial structure is:

$$\mathbf{B}'(\mathbf{x}_B, \sigma) = \mathbf{B}(\mathbf{x}_B, \sigma)\, p(\mathbf{x}_B, \sigma) \tag{8}$$

True contribution to medialness at position $\mathbf{x}_A$ is:

$$m'(\mathbf{x}_A, \sigma) = \left\| \mathbf{B}'(\mathbf{x}_B, \sigma) \right\| \tag{9}$$

3.3 Medialness

The refined medialness at position **x** is the integral of the boundariness contribution to the true medialness structure in the area $O_{\mathbf{x}}^R$ centred at **x** is:

$$M(\mathbf{x}, \sigma) = \int_{O_{\mathbf{x}}^R} m'(\mathbf{v}, \sigma) G(\mathbf{v} - \mathbf{x}, r')\, d\mathbf{v} \tag{10}$$

Where $r' = \lambda\sigma$ (λ is a constant of proportionality which controls the sharpness of the medialness response and has a typical value of 0.5). Here a Gaussian distance weighting function is used to define the region of integration. The extent of this area is defined by setting $R = 3r'$ because a Gaussian function is close to zero at a distance of more than three times its standard deviation.

As proved in [8] that, if N boundary points b_i, $i = 1, \ldots N$ contribute to a medial point A, the medialness response at point A is:

$$M_{CMAT}(\mathbf{x}_A, \cdot) = \left(1 - \frac{1}{N}\right) Sc \tag{11}$$

where S is the sum of the contributions b_i, and c is 1-normalised variability of b_i. The smaller the variability, the more concordance (greater c) exists among the contributions and the greater the medialness is; hence the name: Concordance-based Medial Axis Transform (CMAT).

4 Performance of CMAT

4.1 Medialness Distribution in Scale Space

The CMAT medialness response, like that of HMAT, is a manifold in scale space. For a 1-D structure, the medialness is maximal at the centre of an object when the scale of the medialness operator is optimal (proportional to the width of the object). For a 2-D structure a ridge of medialness is formed along the medial axis positions and at a range of scales corresponding to local widths. This means that it is possible to localise the medial axis accurately at optimal scales by using the HMAT and CMAT algorithms. The LoG operator was criticised by Morse [5] because differences in boundariness strength can change the location of the medialness maximum.

We apply the LoG, HMAT and CMAT medialness algorithms to the 1-D object profile, shown in Fig. 2(a), which corresponds to a dark "object" in a lighter background. The height of the right edge is double that of the left edge. Although the

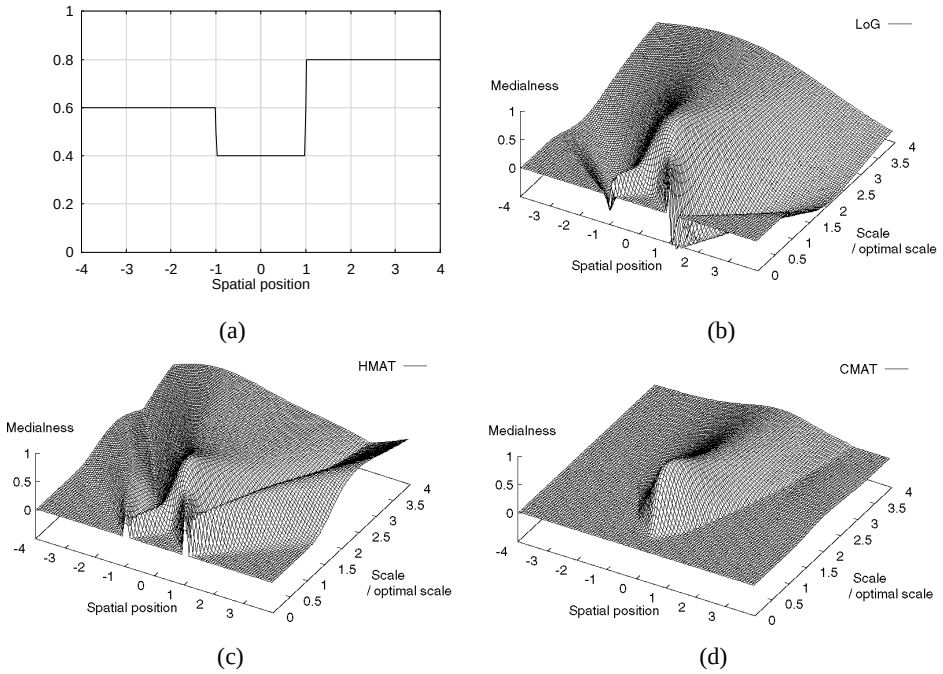

Figure 2: A 1-D object profile (a), and its scale-space surface of medialness from the LoG (b), HMAT (c) and CMAT (d).

quantitative relation between the heights of these two edges is arbitrary, the notion of varying boundary response in grey-level images is represented. The spatial position is normalised by the "width" (half-distance between two edges) of the "object". For medialness responses in scale space, the scale is also normalised by the optimal scale so that the responses of the LoG, HMAT and CMAT algorithms can be compared. Our computation shows that the optimal scale of the LoG is the "width" of the object, while that of the HMAT and CMAT is the half-width. Each medialness response is normalised by its maximum across scale.

Fig. 2(b)-(d) show the two-dimension scale space surfaces for the LoG, HMAT and CMAT medialness responses to the object in Fig. 2(a). The evolution of the LoG and HMAT medialness at increasing scale is similar to the summation of two "waves" "propagating" from the object boundary. The "wave" on one side is sensitive to bright objects on a darker background, and the other is sensitive to dark objects on a brighter background. At a small scale, far from the optimal value, the medialness responses of the LoG and HMAT is strong while the CMAT produces no response. As scale increases, the inward "wavefronts" of the LoG and HMAT begin to "interfere", and produces a response that is not indicative of medialness nor close to the "object" centre. Only the CMAT produces a true medialness response at the object centre. At optimal scale, all three algorithms produce their maximal responses at the object centre. When the scale is larger than the optimal scale, the medialness response of each algorithm begins to collapse. The medialness scale-spaces of the LoG and HMAT are the mixture of boundary and medial properties, while that of the CMAT reflects only medial

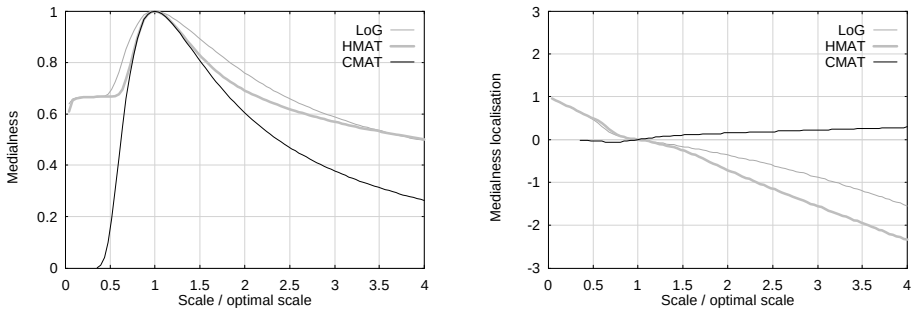

(a) (b)

Figure 3: The magnitude (a) and position (b) of medialness maxima at each scale for the LoG, HMAT and CMAT.

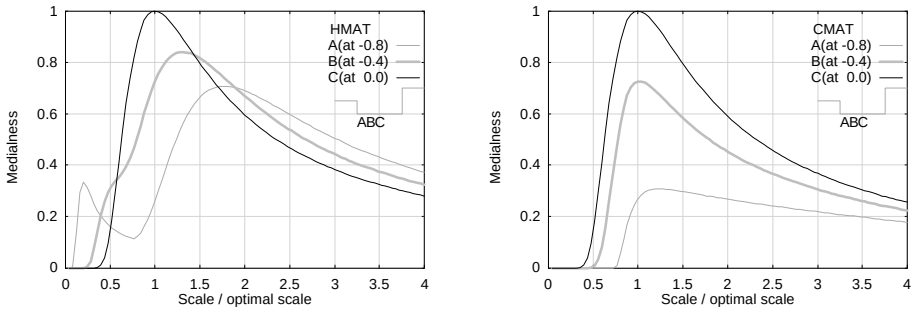

(c) (d)

Figure 4: The medialness response of the HMAT (a) and CMAT (b) across scales at three positions.

properties and therefore provides a clear description of medialness.

Fig. 3(a) shows the maximal responses at each scale for the LoG, HMAT and CMAT medialness. All three medialness estimators give their maximal responses at the optimal scale. Therefore we can accurately localise the medial point using any of these algorithms. The sequence of selectivity to the optimal scale (best first) is: CMAT, HMAT and LoG; the CMAT has a much better scale selectivity than the HMAT and LoG because its response at other than the optimal scale is greatly reduced.

Fig. 3(b) shows the position of maximal responses at each scale for the LoG, HMAT and CMAT medialness estimators. Each trace crosses the object centre at the optimal scale, and then deviates from the object centre almost linearly with scale. The sequence of accuracy of each estimator at a range of scales (best first) is : CMAT, LoG and HMAT. At four times the optimal scale, the localisation bias of the CMAT is 13% that of the HMAT and 19% that of the LoG. This result also shows that, contrary to Morse's conclusion, the HMAT medialness response is more readily moved to one side by differences in boundary strength than the LoG medialness. Despite their obvious difference at non-optimal scales, we can observe that each medialness estimator has a similar localisation bias near the optimal scale.

In order to construct "the optimal scale medialness" for axis extraction, Fritsch

located all medialness extrema across scale for each spatial position [3]. Fig. 4(a)-(b) shows the HMAT and CMAT medialness responses across scale for three points along

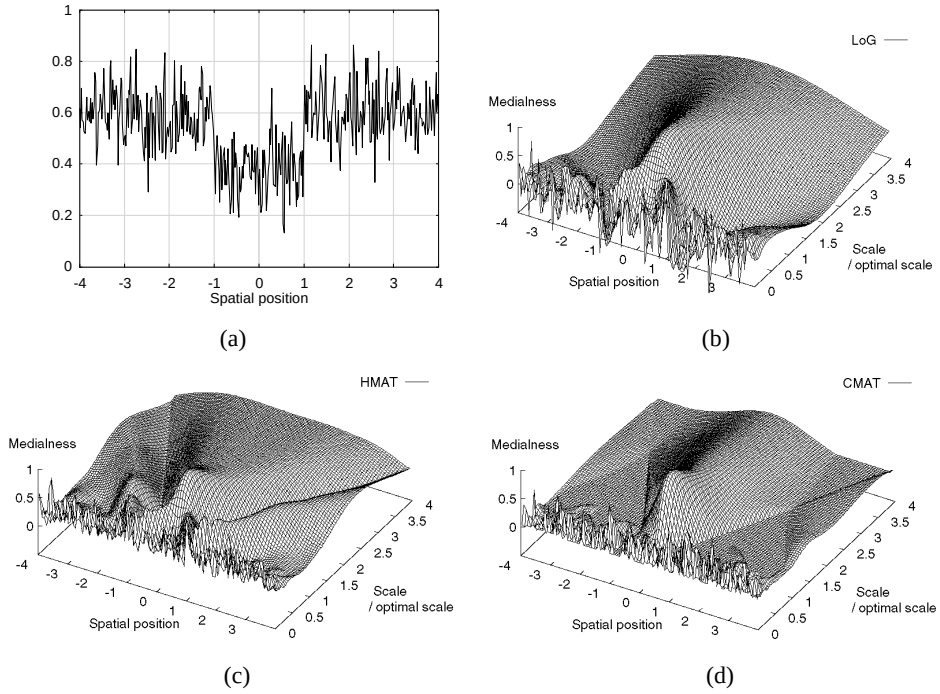

Figure 5: A 1-D noisy object profile, and its scale-space surface of medialness from the LoG (b), HMAT (c) and CMAT (d).

the object. Point A is near a boundary, point C is at the object centre, and B is between A and C. The response for the LoG is similar to that of the HMAT. For positions away from the object centre, both the HMAT and CMAT medialness responses collapse and exhibit medialness extrema at a larger scale than the optimal scale. The scale of medialness extrema for the CMAT is much closer to the optimal scale than that of the HMAT (24% larger than the optimal scale for the CMAT and 76% for the HMAT at point A), which shows that the CMAT is a better estimator of the optimal scale at a position off the object centre. Moreover, the CMAT medialness for the positions off the object centre collapse much faster than the HMAT medialness estimators, which shows that the CMAT has a better selectivity to the object centre than the HMAT. For positions near to the boundary, the HMAT response contains two peaks, while the CMAT response has only one. The first peak of the HMAT response for point A does not represent a true medial property and is an artefact. We can also observe that the CMAT response over scales at the object centre almost coincides the HMAT response.

4.2 Effect of Noise on Medialness

We have tested the LoG, HMAT and CMAT algorithms using a 1-D object under noisy

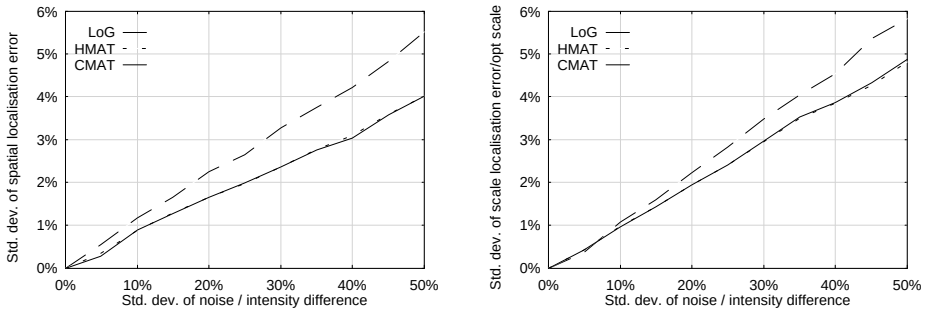

(a) (b)

Figure 6: The standard deviation of spatial (a) and scale (b) localisation error under increasing noise levels.

condition to see how noise affects the computation of medialness. Fig. 5(a) shows an object profile with two boundaries of the same strength, to which Gaussian-distributed noise has been added. The standard deviation of this noise is 50% of the signal amplitude.

Fig. 5(b)-(d) shows the 2-D scale space surfaces of the LoG, HMAT and CMAT medialness responses for the profile in Fig. 5(a). The responses are normalised by the medialness maximum across scale of this profile but without noise. Each the medialness response forms a maximum near the object centre and near the optimal scale, for the primary object. Due to the low level of added noise, medialness response is mainly altered at small scales. As scale increases, its effect greatly decreases and the object medial point can be readily extracted from the scale space. The response surface of the LoG is smoother than those of the HMAT and CMAT, because the LoG uses a double-sized smoothing operator.

Fig. 6(a) and (b) are the standard deviation of spatial and scale localisation errors of the LoG, HMAT and CMAT under increasing noise levels. They are computed over 1000 noisy object profiles for each level of noise. The medial point is realised as the maximal medialness point with a spatial position between [-0.5,0.5] and a scale between [0.7,1.5]. The results show that the standard deviation of spatial and scale localisation error of the LoG, HMAT and CMAT all increase linearly with the standard deviation of noise level. The curves for the CMAT coincides with those for the HMAT, which shows again that these two algorithms have similar performance near the object centre and the optimal scale. The HMAT and CMAT have a 27% lower spatial localisation error and a 15% lower scale localisation error than the LoG.

4.3 Application to Grey-level Images

We applied the HMAT and CMAT algorithms to both synthetic and medical images. Fig. 7(a) is a rectangle with a sawtooth edge, which can be thought of as a primary shape (rectangle) disturbed by fine detail (the sawteeth). The hierarchy and robustness of multiscale analysis are demonstrated: the boundariness and the medialness responses reflect the triangular sawteeth and corner ends at small scales (see Fig. 7(b),(c) and (d)), the rectangle at medium scales (see Fig. 7(e), (f) and(g)), and the elongated shape at

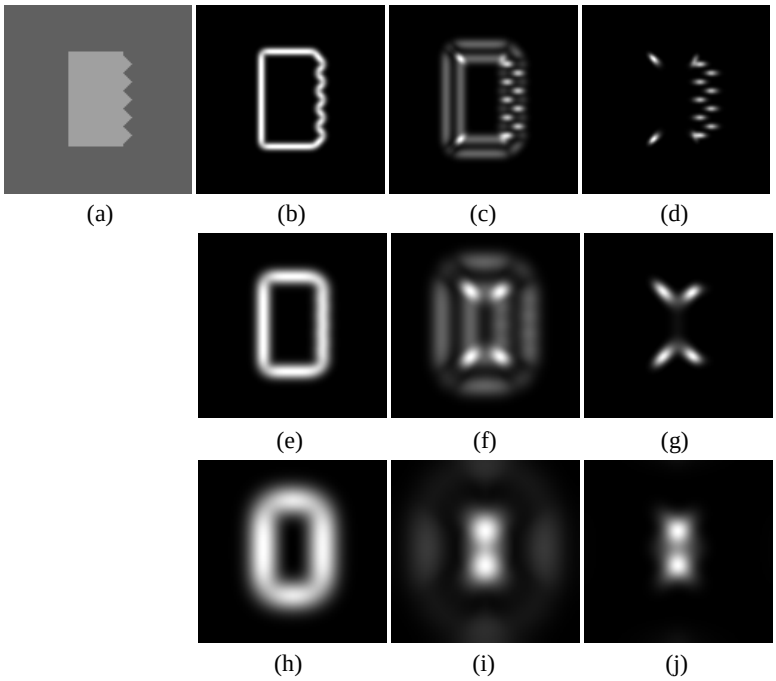

Figure 7: A comparison of medialness response for a rectangle with a sawtooth edge at multiple scales. (a) Original image, (b) boundariness at scale of 2.5 pixels, (c) HMAT medialness at scale of 2.5 pixels, (d) CMAT medialness at scale of 2.5 pixels, (e) boundariness at scale of 5 pixels, (f) HMAT medialness at scale of 5 pixels, (g) CMAT medialness at scale of 5 pixels, (h) boundariness at scale of 10 pixels, (i) HMAT medialness at scale of 10 pixels, and (j) CMAT medialness at scale of 10 pixels.

large scales (see. Fig. 7(h), (i) and (j)). The representation of larger scale properties is little affected by fine detail. The brightest regions of the HMAT medialness response in Fig. 7(c), (f) and (i) correspond to true medial structures whilst the lines framing the shape are spurious responses. On the other hand, all the true medial structures and only the true medial structures are clearly visible in the responses of the CMAT algorithm shown in Fig. 7(d), (g) and (j).

Fig. 8(a) shows an X-ray image of a hand. This image was chosen as an example of a natural image in which the amplitude and sharpness of the grey-level boundary varies, where the shapes are relatively complex and multiple "objects" are in close proximity. As in the synthetic images the CMAT produces a truer representation of medialness which is not confused by the spurious responses shown in the HMAT results. Both internal and external symmetries are clearly visible around the fingers for the CMAT results (see Fig. 8(d)). It can be observed that the fingers are reflected in the medialness as well as boundariness at small scales (see Fig. 8(b), (c), and (d)), and the wrist is reflected at larger scales (see Fig. 8(e), (f) and (g)). The CMAT medialness includes all the true medial structures but gives a clearer description.

5 Conclusions

We have presented the properties of, CMAT, an algorithm for computing the multiscale medial response of grey-level images. The result gives a clearer description of shapesthan previously reported transforms, but maintains localisation accuracy for medial axes and object scale. The elimination of "spurious" medialness responses simplifies the interpretation of the medial transform. Besides this, our approach gives a more selective response to the position and scale of the medial axis. Moreover, the CMAT has a better estimate of medial axis position at other than the optimal scale, and a better estimate of object scale at other than the medial position. The effectiveness of the CMAT is accredited to the use of the concordance measure among boundary contributions.

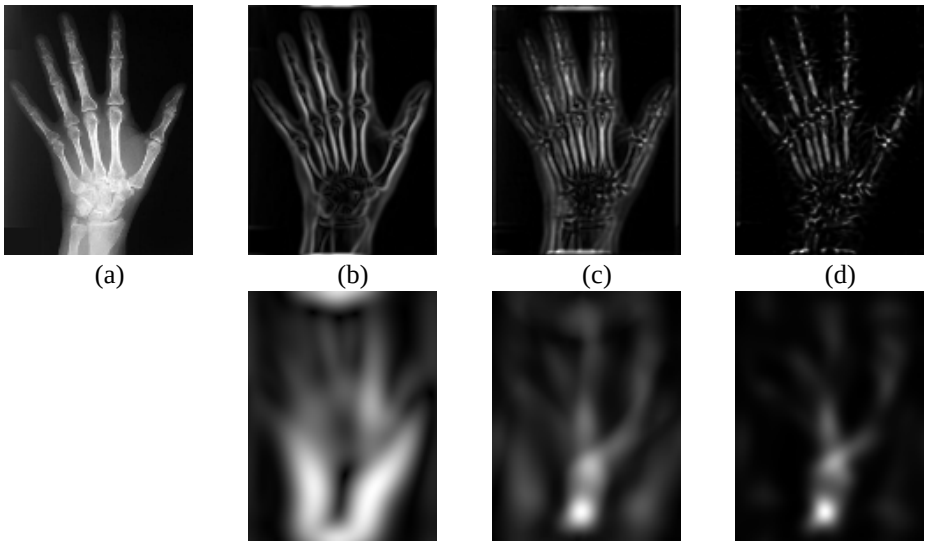

Figure 8: A comparison of medialness response for an X-ray image of a hand. (a) The original image, (b) the boundariness at scale of 1 pixel, (c) the HMAT medialness at scale of 1 pixel, (d) the CMAT medialness at scale of 1 pixel, (d) the boundariness at scale of 8 pixels, (e) the HMAT medialness at scale of 8 pixels, and (g) the CMAT medialness at scale of 8 pixels.

References

[1] H. Blum, A transformation for extracting new descriptors of shape, in *Models for the perception of speech and vision forms* (W. Wathen-Dunn, ed.), MIT Press, 1967, pp. 362-380.

[2] J. L. Crowley and A. C. Parker, A representation for shape based on peaks and ridges in the difference of low-pass transform, *IEEE Transaction on Pattern Analysis and Machine Intelligence*, Vol. 6, pp. 156-169, 1984.

[3] D. S. Fritsch, “Registration of radiotherapy images using multiscale medial descriptions of image structure”, *Ph. D. Dissertation*, Dept. of Biomedical Eng., Univ. of North Carolina, 1993.

[4] J. J. Koenderink and A. J. Doorn, “Dynamic shape”, *Biological Cybernetics*, vol. 53, pp. 383-396, 1986.

[5] B. S. Morse, S. M. Pizer and A. Liu, Multiscale medial analysis of medical images, *Image and Vision Computing*, Vol. 12, pp. 327-338, 1994.

[6] S. M. Pizer, C. A. Burbeck, J. M. Coggins, D. S. Fritsch and B. S. Morse, Object shape before boundary shape: scale-space medial axes, *Journal of Mathematical Imaging and Vision*, Vol. 4, pp. 303-313, 1994.

[7] S. M. Pizer, D. S. Fritsch, V. E. Johnson, and E. L. Chaney, Segmentation, registration, and measurement of shape variation via image object shape, submitted to *IEEE Transaction on Medical Imaging*.

[8] M. Xu and D. Pycock, Estimating true symmetry in scale space, to appear in *Proc. 1998 IEEE International Conference on Systems, Man, and Cybernetics*.